



OPEN

Parametric study and process modeling for metronidazole removal by rhombic dodecahedron ZIF-67 crystals

Sajad Mazloomi^{1,2}, Ali Amarloei^{2,3}, Faeze Gholami⁴, Gholam Ali Haghghat^{5,6}, Gagik Badalians Gholikandi⁵, Heshmatollah Nourmoradi^{2,3}, Ali Akbar Mohammadi⁷✉, Mehdi Fattahi^{8,9}✉ & Binh Nguyen Le^{8,9}

Metronidazole (MNZ) is an extensively used antibiotic against bacterial infections for humans and farm animals. Prevention of antibiotics discharge is essential to prevent adverse environmental and health impacts. A member of metal–organic frameworks, zeolite imidazole framework-67 with cobalt sulfate precursor (ZIF-67-SO₄) and exceptional physio-chemical properties was prepared via room temperature precipitation to adsorb MNZ. The study framework was designed by Box–Behnken Design to evaluate the effect of pH, ZIF-67-SO₄ dose, and contact time on adsorption efficiency. The polynomial model fitted the adsorption system indicated the optimal condition for 97% MNZ removal occurs at pH = 7, adsorbent dosage = 1 g/L, and mixing time = 60 min. The model also revealed that the removal increased with contact time and decreased at strong pH. Equilibrium and kinetic study also indicated the adsorption of MNZ followed the intra-particle diffusion model and the Langmuir isotherm model with a q_{max} = 63.03 mg/g. The insignificant loss in removal efficacy in use-reuse adsorption cycles reflected the practical viability of ZIF-67-SO₄.

Metal–organic frameworks (MOFs) are a new class of materials consisting of metal ions or clusters coordinated with organic ligands to form one-, two-, or three-dimensional structures¹. The open frameworks in MOFs made them unique materials with extraordinary properties such as permanent porosity, stable framework, enormous surface area, and pore volume². MOFs attracted significant attention in recent years due to their unique properties and potential applications in various fields³. MOFs have a high surface area and tunable pore size, which makes them attractive for gas storage and separation. They have also been used for catalysis, drug delivery, sensing and energy storage applications⁴.

Zeolitic imidazolate frameworks (ZIFs) are a type of MOF that have been extensively studied due to their high thermal and chemical stability, tunable pore size, and high catalytic activity. ZIF-67 is a cobalt-based MOF that has been used for various applications such as adsorption, separation, electrochemistry, and catalysis. It also has been used as adsorbent for extracting herbicides in aqueous samples in the solid-phase microextraction (SPME) technique⁵, and as a catalyst for the condensation reaction of benzaldehyde with nitromethane. The structural, and electrical properties of ZIF-67 made it interesting material for the synthesis of catalysts and heterojunctions^{6–8}.

The morphological evolution of Co-MOF-based ZIF-67 was investigated in the literature by changing the reaction conditions, including the cobalt source, type of solvent, aging time, crystallization temperature, and organic linker for the cobalt ions⁶. ZIF-67 prepared by cobalt sulfate has interesting physical and chemical properties

¹Biotechnology and Medicinal Plants Research Center, Faculty of Medicine, Ilam University of Medical Sciences, Ilam, Iran. ²Department of Environmental Health Engineering, School of Public Health, Ilam University of Medical Sciences, Ilam, Iran. ³Health and Environment Research Center, Ilam University of Medical Sciences, Ilam, Iran. ⁴Department of Environmental Health Engineering, School of Public Health, Iran University of Medical Sciences, Tehran, Iran. ⁵Faculty of Civil, Water and Environmental Engineering, Shahid Beheshti University, Tehran, Iran. ⁶Department of Environmental Health Engineering, School of Health, Jiroft University of Medical Sciences, Jiroft, Iran. ⁷Department of Environmental Health Engineering, Neyshabur University of Medical Sciences, Neyshabur, Iran. ⁸Institute of Research and Development, Duy Tan University, Da Nang, Vietnam. ⁹School of Engineering & Technology, Duy Tan University, Da Nang, Vietnam. ✉email: mohammadi.eng73@gmail.com; mehdfattahi@duytan.edu.vn

that make it an excellent candidate for various applications such as adsorption of volatile organic compounds (VOCs), separation, supercapacitors, and catalysis.

The choice of metal source is critical in the synthesis of Zeolitic Imidazolate Frameworks (ZIFs) as it affects the morphology and physicochemical properties of the product⁹. For instance, using $\text{Co}(\text{NO}_3)_2$ as a cobalt source results in small-sized and agglomerated ZIF-67 crystals. On the other hand, small-sized rhombic dodecahedron crystals were obtained when CoCl_2 was introduced in the synthesis solution. Likewise, large-sized crystals of rhombic dodecahedron structure were obtained by the application of CoSO_4 and $\text{Co}(\text{OAc})$ salts¹⁰. The flexible and engineerable structure of ZIFs and other MOFs make them attractive target materials in environmental remediation such as water treatment.

Water is an indispensable environmental resource for all forms of life. However, the contamination of water has become a major environmental hazard for humans and other living species. The extensive use of antibiotics has been associated with the contamination of various compartments of the environment such as surface water, groundwater, drinking water, municipal sewage, soil, vegetables, and sludge¹¹. The release of antibiotics by antibiotic manufacturers discharges, animal farming, and hospital wastewater is a significant concern for human health and the environment^{12,13}. Many antibiotics are classified as refractory chemicals with potential mutagenicity, and carcinogenicity¹⁴. In particular, metronidazole (MNZ) is a widely used antibiotic against bacterial infections in humans and farm animals. The conventional treatment techniques are inefficient in abating MNZ as it is highly soluble in water and also has a very robust chemical structure. MNZ can accumulate in the human body and the environment due to its recalcitrant nature. Encephalopathy, seizures, cerebellar, and spinal cord damage are among the harmful effects of MNZ ingested by drinking water^{15,16}.

Of different pollutant removal techniques, adsorption is nominated as a convenient, economical, and friendly practice. This is due to the simple design and operation of the system, flexibility of adsorbent materials for different contaminants, reusability of materials, and efficiency of the process special in low levels of pollutants. Despite drawbacks such as requiring adsorbent regeneration, adsorption is still an advantageous treatment technique that produces minimal sludge and polluted streams that are hard to handle^{17,18}.

The adsorption of metronidazole from aqueous media has been studied to reduce its pollution in water bodies. Kalhorizadeh et al.¹⁹ conducted a study on MNZ removal using two model metal–organic frameworks (MOFs), namely NH 2-MIL-101-Fe and HKUST-1. The authors concluded that both MOFs are effective in removing MNZ and NH2-MIL-101-Fe was identified as a superior adsorbent compared to HKUST-1.

Seo et al. reported MIL-101 (Cr) modified with urea or melamine for improved removal of nitroimidazole from water²⁰. In another study, eight water-stable MOFs were screened for the removal of MNZ from water. The authors reported that two isostructural Zr (IV)-MOFs ($\text{UiO}-66$ and $\text{UiO}-66\text{-NH}_2$) have a promising adsorption efficacy for MNZ²¹. In another study, ZIF-8 was synthesized and used for the removal of MNZ from water. The authors reported the MNZ removal in optimal condition predicted by the quadratic model reached to a high percentage of ~94%²².

Due to the unique properties i.e., uniform crystals, structural robustness, facile and environmentally friendly preparation method in aqueous medium, and high-yield production, ZIF-67- SO_4 was investigated in this study as a viable material for MNZ removal. The key physicochemical parameters such as contact time, adsorbent mass, pH, and MNZ concentration were experimented to understand their impacts on the sorption system. Box–Behnken design (BBD), a particular technique of response surface methodology (RSM) that uses a statistical approach to design the experiments in three parametric levels was used to develop a mathematical model. The model provided an in-depth view on the process, and a tool to optimize the process for the highest removal, and also to describe the interactions of operating variables on MNZ adsorption.

Materials and methods

Chemicals. Zeolitic imidazolate framework-67 (ZIF-67) is composed of cobalt ions and 2-Methylimidazole (HMIM) linkers. Cobalt sulfate (CoSO_4) was used as a source of metal in ZIF-67. All chemicals used in the synthesis of ZIF-67 and preparation of metronidazole (MNZ) solution were analytical grade and purchased from Merck or Sigma-Aldrich. Deionized (DI) water with an electrical conductivity of less than 0.5 $\mu\text{S}/\text{cm}$ was used throughout the study for the experiments. Acetonitrile (ACN) and DI with HPLC grade were used for measuring MNZ.

Adsorbent preparation. ZIF-67- SO_4 was synthesized at room temperature using a simple precipitation technique described earlier²³. 0.281 g of CoSO_4 was added to a 10 mL solution of deionized water to prepare the metal precursor. A second solution was prepared by adding 1.642 g HMIM to 10 mL DI. To obtain ZIF-67, the two solutions were mixed and stirred for 30 min to complete the formation of crystals. After crystals formed, the precipitates were separated by centrifugation at 5000 rpm, washed with deionized water, and dried at 80 °C overnight.

Adsorption experiments. The adsorption efficacy of ZIF-67- SO_4 was evaluated in a batch mode operation system by MNZ (25 mg/L) as the contaminant of interest. The samples were mixed using a magnet stirrer at 250 rpm. The temperature (23 ± 1 °C) and mixing speed were not changed throughout the experiments. MNZ concentration was determined by high-performance liquid chromatography (HPLC; Knauer smartline, Germany) equipped with a C18 column and UV–VIS detector at 320 nm. For the operation of HPLC, the mobile phase was ACN: WATER in the ratio of 60:40. The experiments were performed twice and the average values were used for data analysis.

BBD modeling and optimization. Response Surface Methodology (RSM) was used to study the effect of operating factors. RSM is a set of statistical and mathematical methods that are used to explore the relationships between several explanatory variables and to optimize one or more response variables result in the desired output. Box–Behnken Design (BBD) is a particular type of RSM that is specially designed to fit a second-order model on the data²⁴. BBD design has the advantage of being highly accurate, easy to implement, and requiring fewer trials compared to other RSM and also one-factor-at-a-time techniques. The variables and the level of each factor in this study are shown in Table 1.

After generating the experimental matrix in Table 2, the sorption experiments were accomplished as ordered in the table and the final MNZ concentration was determined in clear centrifuged solutions. The adsorption removal efficiency for ZIF-67-SO₄ and the capacity of adsorbent (q) for MNZ were responses in this study and calculated by the following equations:

$$\text{Adsorption removal (\%)} = \frac{(C_i - C_t)}{C_i} \times 100 \quad (1)$$

$$q_t \text{ (mg/g)} = \frac{(C_i - C_t) \times V}{m} \quad (2)$$

$$q_e \text{ (mg/g)} = \frac{(C_i - C_f) \times V}{m} \quad (3)$$

where C_i , C_t , and C_f are the concentration of MNZ (mg/L) in the solution before adsorption begins, at any specific time, and the equilibrium, respectively. In the equations, m is the ZIF-67-SO₄ mass (g) and V is the volume of the solution (L), respectively.

The data obtained experimentally were analyzed by Analysis of Variance (ANOVA) to set a polynomial equation describe the process response ($Y = \text{MNZ removal}$) as a function of operating factors i.e., X_i and X_j :

$$Y = \beta_0 + \sum_{i=1}^k \beta_i X_i + \sum_{i=1}^k \beta_{ii} X_i^2 + \sum_{i=1}^{k-1} \sum_{j=i+1}^k \beta_{ij} X_i X_j + \varepsilon \quad (4)$$

where β_0 is a constant value, β_i , β_{ii} , and β_{ij} are the coefficients for linear, second-order, and interaction effects, and ε is the error constant for the model.

Factor	Code	Variable level		
		- 1	0	+ 1
ZIF-67-SO ₄ (g/L)	A	0.25	0.625	1
Mixing time (min)	B	15	37.5	60
pH	C	4	7	10

Table 1. The variables and the level of each factor in this study.

Order	Adsorbent dose g/L	Mixing time min	pH	Removal %
1	1	37.5	4	69
2	0.25	37.5	4	48
3	0.625	60	4	72
4	0.625	15	4	54.8
5	0.25	60	7	76
6	1	60	7	97
7	0.625	37.5	7	94.6
8	0.625	37.5	7	91.6
9	1	15	7	76.9
10	0.25	15	7	68
11	0.625	37.5	7	92.6
12	0.25	37.5	10	61.6
13	1	37.5	10	86.3
14	0.625	60	10	78.6
15	0.625	15	10	73

Table 2. The experimental matrix and corresponding responses for MNZ removal by ZIF-67-SO₄.

Once the model is developed, optimization of the polynomial equation accomplished to determine the best level for each variable in which the highest MNZ adsorption happens. The optimal condition was then validated through the additional experiments.

Isotherm and kinetic studies. Isotherm and kinetic studies are since they assist to realize the behavior of the adsorbent and the mechanism governing the adsorption. Isotherm models mirror the relationship between the mass of adsorbate on adsorbent and its concentration in solution at equilibrium. Kinetic models, on the other hand, are extensively used to determine the rate of adsorption which is an important factor in the economy of the process. The models are crucial in the optimal design and operation of the real treatment unit. In this study, kinetic and isotherm experiments performed in the optimal condition described in optimization section. For the equilibrium study, the concentration of MNZ was studied in the range of 5–50 mg/L.

Langmuir model is a theoretical equation that explains the adsorption of gases onto a solid surface and was proposed in 1916. The Langmuir isotherm assumes that adsorption is limited to a monolayer, the adsorbent surface is homogeneous, and all sorption sites are energetically identical. The Freundlich isotherm, on the other hand, is a mathematical model that describes the multilayer adsorption of a solute onto a heterogeneous adsorbent surface²⁵.

The Temkin isotherm is another popular model in environmental studies. The assumption behind the development of the model is that the adsorption temperature of all molecules decreases as the surface of the adsorbent becomes more covered²⁶. The empirical Redlich–Peterson (R–P) isotherm is commonly used model to describe adsorption in microporous materials.

The pseudo-first-order (PFO) and pseudo-second-order (PSO) kinetic models are common kinetic models to describe the rate of adsorption. The former model describes the adsorption system as proportional to the number of free-binding sites on the surface. The PSO, otherwise, attributed the adsorbate attachment to the surface by the chemical bonding²⁷. The intra-particle diffusion (IPD) model, describes the pollutant migration process from liquid bulk to the adsorbent pores and assumed it as the rate-limiting step in adsorption²⁸. The nonlinear forms of isotherm models are provided in Table S1²⁹.

Results and discussion

ZIF-67-SO₄ characteristics. The as-synthesized ZIF-67-SO₄ was analyzed by scanning electron microscopy (FE-SEM, MIRA3 TESCAN, Czech Republic) to reveal information about the texture morphology and crystalline structure. X-ray diffraction (XRD; Unisantis S.A, XMD300 model, Geneva, Switzerland) using Cu-ka beam was also used for phase identification of crystalline ZIF-67-SO₄. Fourier-transform infrared spectroscopy (FTIR; Thermo Nicolet, Avatar 370), and N₂ adsorption–desorption (BELSORP-mini-II BEL Japan, Inc.) also performed to identify the functional groups, and pore volume/ specific surface area, respectively. Figure 1a shows the SEM image of ZIF-67-SO₄ crystals that have the uniform truncated rhombic dodecahedral framework. The XRD pattern of ZIF-67-SO₄ shown in Fig. 1b shows the major characteristic peaks correspond to the crystallographic planes of the ZIF-67-SO₄ at 7.6, 10.6, 13.1, and 17.9 degrees of 2θ assigned to the (011), (002), (112), and (222) planes, respectively³⁰. The ZIF-67-SO₄ FTIR spectrum in Fig. 1c displays peaks at 3404 cm⁻¹ for N–H stretching, 3128 cm⁻¹ and 2907 cm⁻¹ for C–H stretching from the methyl group on the imidazole ring, a peak at 1572 cm⁻¹ for CN stretching, peaks from 1428 to 667 cm⁻¹ due to the stretching of the imidazole ring, and a peak at 414 cm⁻¹ due to Co–N stretching. These characteristic peaks confirm the bond developed between cobalt and the linker³¹. N₂ adsorption desorption analysis performed and indicated the porous nature of the adsorbent structure. The SSA, total pore volume, and average pore diameter of ZIF-67-SO₄ crystals based on the BET model in Fig. 1d were 737.5 m²/g, 0.322 m³/g, and 1.75 nm, respectively.

MNZ modeling and optimization. BBD design is an interesting statistical approach that conducted to fit a non-linear model on system performance as a function of study variables. In BBD, the number of experimental runs is determined by the following formula:

$$N = 2^K + 2K + 1 \quad (5)$$

In Eq. 5, N is the number of experimental runs, and K is the number of variables. Table 2 presents the study matrix consisting of 15 runs, and responses for each experiment. As seen, the removal efficiencies ranged from 48 to 97%, which are the lowest and highest values recorded experimentally.

The experimental efficiencies were undergoing an ANOVA statistical analysis to fit a polynomial model. The result of the quadratic model fitted to the experimental data is presented in Table 3.

The F-value is an important statistical value that is used to check whether the null hypothesis should be rejected or not. The Model F-value of 37.27 implies it is significant and there is only a 0.05% chance that an F-value this large could occur due to the noise. If the p-value is less than 0.05, it indicates that the model terms in Table 3 are significant. In this case, A, B, C, A², B², C² are significant model terms. The Lack of Fit (LOF) F-value is also a significant statistical value that reflects whether the LOF is significant relative to the pure error. For the developed model, the LOF F-value of 5.62 implies that the Lack of Fit is not significant. The Predicted R² of 0.7864 is in rational agreement (within ± 0.2) with the R²_{Adj} of 0.9589. While R² measures how well a regression model fits the data, the Predicted R² is calculated by a subdivision of the data to predict the residual data. The Adjusted R² is a revised form of R² that used to compare different models with different numbers of predictors as the parameters adjusts for the number of predictors. Another statistical indicator, Adeq Precision, measures the ratio of signal to noise. The value of 19.634 is above the minimum desirable value of 4 and indicates an adequate signal. A polynomial equation was developed based on quadratic model coefficients calculated for coded factors in Table 4.

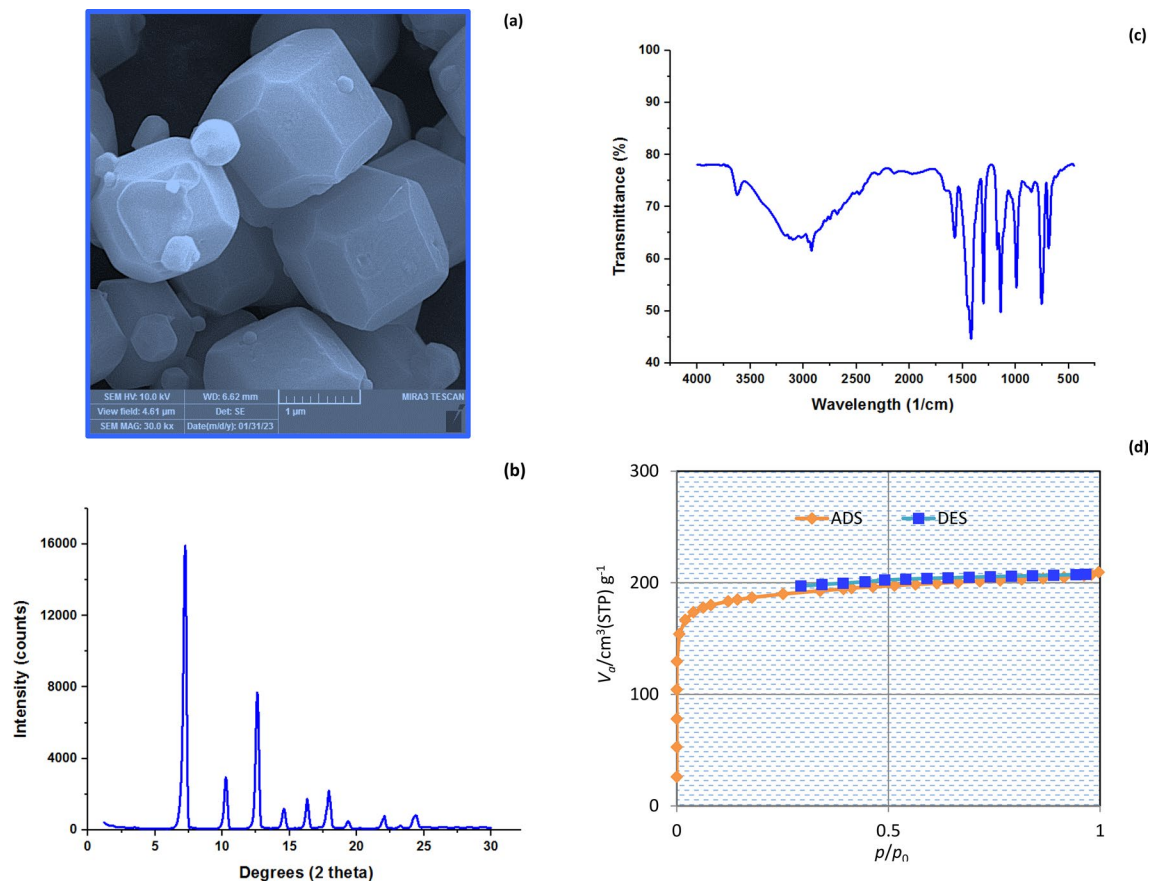


Figure 1. The structural properties of ZIF-67-SO₄, FESEM image (a), XRD pattern, FTIR spectrum, and N₂ adsorption–desorption.

Source	Sum of squares	DF	Mean square	F-value	p value
Model	2954.31	9	328.26	37.27	0.0005
A-dose	714.42	1	714.42	81.12	0.0003
B-time	323.85	1	323.85	36.77	0.0018
C-pH	387.81	1	387.81	44.04	0.0012
AB	36.60	1	36.60	4.16	0.0970
AC	3.42	1	3.42	0.3886	0.5604
BC	33.64	1	33.64	3.82	0.1081
A ²	261.56	1	261.56	29.70	0.0028
B ²	93.85	1	93.85	10.66	0.0223
C ²	1235.39	1	1235.39	140.28	<0.0001
Residual	44.03	5	8.81		
Lack of Fit	39.37	3	13.12	5.62	0.1547
Pure Error	4.67	2	2.33		
Cor Total	2998.34	14			
R ²	0.9853				
Adjusted R ²	0.9589				
Adeq Precision	19.6343				

Table 3. ANOVA for the quadratic model fitted to MNZ removal by ZIF-67-SO₄.

The final model equation based on code, and actual values for the variables are presented in Eqs. (6) and (7), respectively.

Factor	Coefficient Estimate	df	Standard Error	95% CI Low	95% CI High	VIF
Intercept	92.93	1	1.71	88.53	97.34	
A-dose	9.45	1	1.05	6.75	12.15	1.0000
B-time	6.36	1	1.05	3.67	9.06	1.0000
C-pH	6.96	1	1.05	4.27	9.66	1.0000
AB	3.03	1	1.48	-0.7893	6.84	1.0000
AC	0.9250	1	1.48	-2.89	4.74	1.0000
BC	-2.90	1	1.48	-6.71	0.9143	1.0000
A ²	-8.42	1	1.54	-12.39	-4.45	1.01
B ²	-5.04	1	1.54	-9.01	-1.07	1.01
C ²	-18.29	1	1.54	-22.26	-14.32	1.01

Table 4. Coefficients calculated for the quadratic model based on the coded factors.

$$\text{MNZ removal (\%)} = + 92.939.45A + 6.36B + 6.96C + 3.03AB + 0.9250AC - 2.90BC - 8.42 A^2 - 5.04 B^2 - 18.29 C^2 \quad (6)$$

$$\text{MNZ removal (\%)} = - 85.91 + 80.81 \text{ dose} + 1.1 \text{ time} + 31.87 \text{ pH} + 0.35 \text{ dose} \times \text{time} + 0.82 \text{ dose} \times \text{pH} - 0.042 \text{ time} \times \text{pH} - 59.85 \text{ dose}^2 - 0.009 \text{ time}^2 - 2.03 \text{ pH}^2 \quad (7)$$

The Eq. 6 and Eq. 7 could be used as a tool to predict the MNZ removal for given levels of each factor. The coded equation (Eq. 6) provides a useful tool to identify the relative impact of each factor by comparing the factor coefficients. Accordingly, the adsorbent mass (A) has the highest coefficient in the model and hence the highest impact on the process. The equation in terms of actual factors (Eq. 7) can be used to predict the response for given levels of each factor in the original units.

Effect of study variables. One essential part of the sorption study is analyzing how contaminants are removed as a function of operating variables. BBD design is a powerful tool to explain how independent factors and their interactions affect the process. ZIF-67-SO₄ dose, pH, and mixing time were considered as independent variables for MNZ removal. 3D plots that were developed based on the Eq. 5. were used to illustrate how MNZ removal was changed by operating conditions.

Figure 2a shows the effect of pH and mixing time on the process. The pH of the solution can affect the charge of the adsorbent and ionic state of MNZ, so it has a significant effect on the process. The figure shows the antibiotic removal reached a maximum value at pH ~ 8. The pH_{ZPC} for the ZIF-67 was determined ~ 9.8 which means the crystal's surface charge changed over different solution pH. Once the solution pH is < 9.8, the surface charge of the adsorbent becomes positive. A negative surface charge developed by increasing pH from 9.8. Changes in adsorbent surface charge directly impact MNZ removal by developing attraction or repellent electrostatic force. The pKa1 and pKa2 for MNZ as a weak base are 2.38 and 14.48, respectively. At pH > 4, MNZ has a positive charge as it is protonated in the solution. At pH 4–12, and pH > 12, MNZ is neutral and negatively charged since it is de-protonated by pH. The repelling electrostatic force by domination of positive surface charge and positive MNZ in the acidic environment, and negative surface charge of ZIF and anionic MNZ at alkaline conditions are responsible for removal drop. Furthermore, at the higher pH, the presence of OH⁻ also hinders MNZ ions to attach the adsorbent^{29,30}. Lower MNZ adsorption in acidic condition, on the other hand, could be attributed to the net repulsive force that exists between the positive species MNZ⁺, H⁺, and ZIF-67⁺. Alamgir et al.²¹ studied MNZ removal and found a good adsorptive removal by UiO-66-NH₂ in a wide range of pH from 4 to nearly 8. They attributed the adsorption to the development of electrostatic interaction and hydrogen bonding. Other studies also indicated that hydrogen bonding plays a critical role in the adsorption performance of MOFs due to the presence of functional groups³². Mixing time also is imperative variable in sorption systems as it provides the time required for contaminants to diffuse toward the adsorbent. Mixing time is also important for the economy of a treatment unit as it determines the volume required for the reactor. The figure shows a rapid uptake of ~ 50% MNZ at the initial 15 min which gradually increased by mixing time to 60 min. Zeng et al.³³ conducted a study on Doxycycline and Ciprofloxacin adsorption by biochar and found a rapid uptake of antibiotics in the first 30 min of the adsorption which gradually increased with time. Alsaedi et al.³⁴ conducted another study that showed the maximum removal of Doxycycline by UiO-66 happened within 15 min. Zong et al.³⁵ also reported a steep slope and a straight regression line in the first part of the tetracycline (TC) and ciprofloxacin (CIP) adsorption by Zr-MOFs, indicating a fast adsorption. The second part of the kinetic model had a gradual slope, indicating that the adsorption equilibrium changed slowly with time. The effect of ZIF-67-SO₄ dose in the range of 0.25–1 g/L is presented in Fig. 2b. As seen, MNZ removal increased by the mass of adsorbent added to the solutions. Higher adsorbent mass result in a higher adsorption efficiency in many earlier studies. Elkady et al.³⁶ prepared an environmentally friendly zirconium Bio-MOF for trimethoprim antibiotic. The parametric study of antibiotic removal showed increasing the MOF dose from 0.1 to 1.5 g/L increased the removal from 47.7 to 87.6%, respectively. In another study, MNZ removal by polypyrrole studied as a function of dose in the range of 0.05–0.70

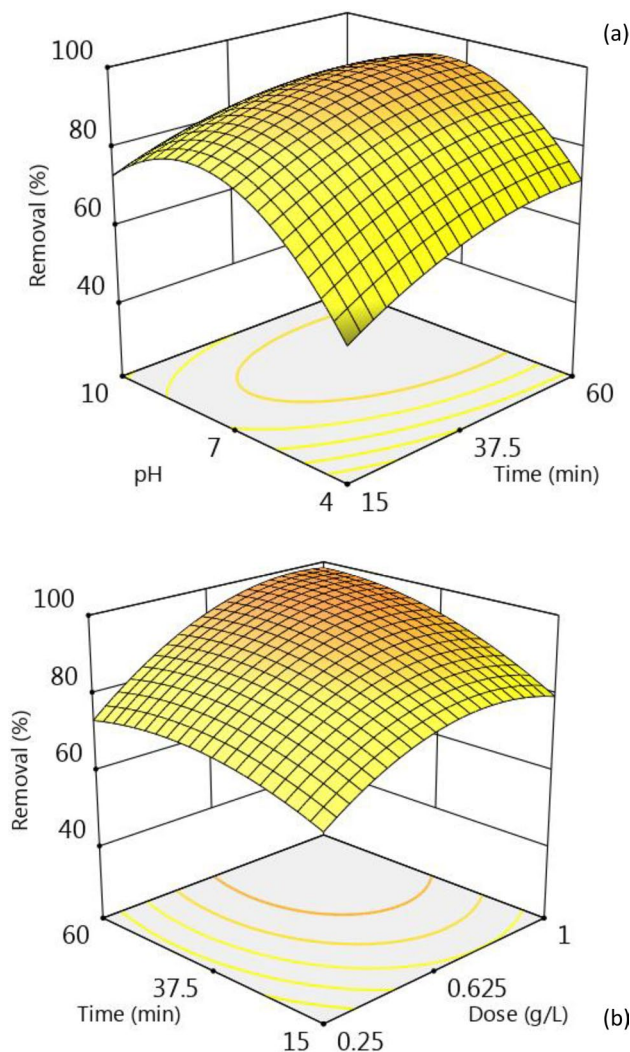


Figure 2. The 3D plots for the effect of independent variables on MNZ removal by ZIF-67-SO₄.

g/L. The authors reported an incremental removal by dose from about 60 to 89.55% when the dosage increased above 0.5 g/L. The optimal adsorbent dose of 0.5 g/L finally chosen based on the economic considerations³⁷.

Model optimization and validation: Model optimization and validation are crucial in adsorption because they help to assure the model predict the response with adequate preciseness. Optimization also useful to identify the best operating condition for the best performance³⁸. Herein, the model presented in Eq. 5 was solved for the highest MNZ removal and the graphical representation showed in Fig. 3. The highest MNZ removal of ~97% was achieved when pH=7, adsorbent dosage=1 g/L, and mixing time=60 min. This condition was simulated and experimented to check the validity of the model optimization. The average antibiotic removal by three replications was 95.8 which is close that predicted by the model.

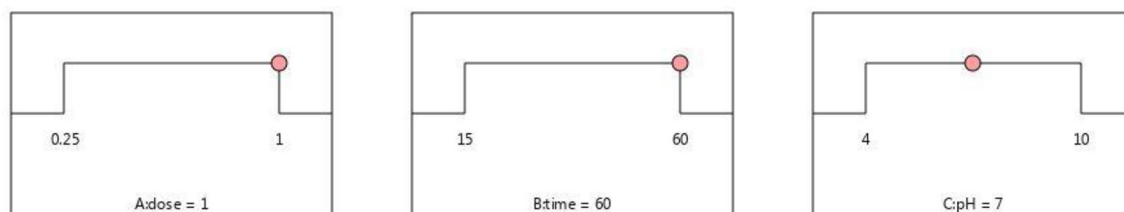


Figure 3. Graphical representation for the highest MNZ removal by ZIF-67-SO₄.

Effect of MNZ concentration. Once the optimum levels of operating parameters determined, the process was studied as a function of MNZ concentration. Solutions of different antibiotic concentrations in the range of 5–50 mg/L were prepared and adsorption experimented in the presence of 1 g/L ZIF-67-SO₄, and solution pH=7. MNZ removal calculated at different time intervals and the results are presented in Fig. 4. As seen, ZIF-67-SO₄ showed a significant adsorption property over a wide range of antibiotic concentrations, and up to 90% removal observed for the concentration of 25 mg/L. The graph also reveals the adsorption decreased from ~99 to ~76% when MNZ concentration increased in the studied range. A higher competition for limited adsorption sites on the surface is the possible cause of removal drop as also described in earlier works^{9,39}.

Effect of temperature. The temperature is an important variable is sorption of contaminants as it determines the diffusion rate of contaminants and also the adsorbent-adsorbate bonds. MNZ removal under optimum condition i.e., pH=7, adsorbent dosage=1 g/L, and mixing time=60 min was studied as a function of temperature to realize the effect of solution temperature on the process. The study indicated that the MNZ removal decreased from ~96% in 23±2 °C to about~88% in 45±2 °C that is an indication of exothermic adsorption. Different behavior in adsorption of MNZ reported for studied adsorbents. Sun et al. and Arbab et al. indicated the MNZ antibiotic adsorption onto biochar derived from Sugarcane Bagasse, and polypyrrole, respectively, is exothermic^{37,40}. Nasseh et al.⁴¹ on the other hand, indicated the MNZ removal by FeNi₃/SiO₂/CuS magnetic nanocomposite increased from 37.73 to 65.15% as the temperature elevated in the studied range.

Kinetic and isotherm studies. Kinetic and isotherm studies are important in adsorption because they provide valuable information about the adsorption process, the potential rate-limiting phase, and economy of treatment which can be used to optimize the design of adsorption systems and improve their efficiency⁴². The results of isotherm modeling in Table 5 shows the Sips model fit best on equilibrium data. Sips model is widely used to describe the adsorption of a solute onto a solid surface at a fixed temperature. This theoretical model derived from the limiting behavior of the Langmuir and Freundlich isotherms and assumed that MNZ adsorption onto ZIF-67-SO₄ occurred on localized specific sites. In addition, the model suggested that there is no interaction between adsorbed MNZ molecules^{43,44}.

The maximum monolayer adsorption capacity (q_{max}) of ZIF-67-SO₄ for MNZ was 63.03 mg/g which is an essential tool to compare different adsorbents. Table 6 listed the q_{max} of ZIF-67-SO₄ and other adsorbents studied against MNZ. As seen, ZIF-67-SO₄ and other MOFs are generally promising materials with significant capacities for MNZ. A significant improvement also is attainable by preparing composites and modified forms of MOFs that indicated the versatile and engineerable nature of these emerging materials.

Table 7 listed the non-linear kinetic models and related parameters for MNZ removal by ZIF-67-SO₄. As seen, the data fit to the Pseudo-first order (PFO), pseudo-second order (PSO), and intra-particle diffusion (IPD) models. The data also illustrated graphically and presented in Fig S1. As seen, the IPD model fit best with non-linear model. According to IPA, the adsorbate diffusion inside the pores proposes as the rate-limiting step in the overall adsorption process^{47,48}.

Reusability tests. The regenerability of the adsorbents for adsorption–desorption cycles is a substantial feature that determines the economic and environmental viability of the sorption system. Hence, studying the adsorbent behavior at consecutive use-reuse series is of practical significance. Once pristine ZIF-67-SO₄ was saturated with MNZ, desorption was accomplished by soaking the material in ETOH for 24 h while ETOH was replaced with the fresh solution every 4 h. ZIF-67-SO₄ was finally washed thoroughly with deionized water and dried overnight for the next cycle. The reusability tests were accomplished at optimal conditions predicted by the model i.e., pH=7, adsorbent dosage=1 g/L, and mixing time=60 min. Figure 5 indicated the MNZ removal

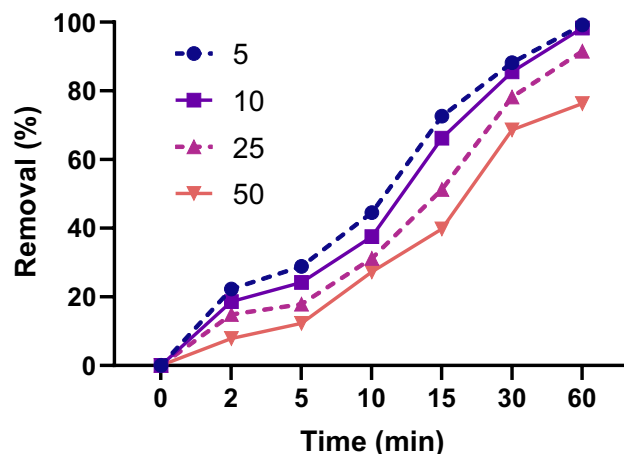


Figure 4. MNZ removal by ZIF-67-SO₄ as a function of antibiotic concentration (ZIF-67-SO₄: 1g/L, pH=7).

Langmuir	q_{\max} (mg/g)	62.40
	K_L (L/mg)	1.64
	R^2	0.99
	R^2_{adj}	0.98
	RSS	28.09
Freundlich	K_F (mg/g) (L/mg) ^{1/n}	30.33
	n	3.44
	R^2	0.97
	R^2_{adj}	0.96
	RSS	67.27
Temkin	A_t	23.56
	bT_1	9.58
	R^2	0.99
	R^2_{adj}	0.98
	RSS	19.67
Dubinin–Radushkevich	kRP (mg/g)	191.24
	aRP	4.29
	R^2	0.99
	R^2_{adj}	0.99
	RSS	2.42
Sips	qms	71.06
	KS	1.02
	Ms	0.69
	R^2	0.99
	R^2_{adj}	0.99
	RSS	1.33

Table 5. The isotherm parameters for MNZ removal by ZIF-67-SO₄.

MOF	Qmax (mg/g)	Reference
AgN/MOF-5	191.1	45
UiO-66-NH ₂	265.5	21
Chitosan-Modified Graphene Oxide	29.76	46
polypyrrole (PPy)	5.05	37
Urea-MIL-101	188	20
ZIF-8	30	22
Cu-ZIF-8	16	
ZIF-67-SO ₄	62.40	This study

Table 6. Qmax of ZIF-67-SO₄ and other adsorbents for MNZ.

decreased from 96.3% for pristine adsorbent to ~78.6% for the 3rd cycle. The insignificant loss in removal efficacy reflected the practical usability of ZIF-67-SO₄.

MNZ removal mechanism. ZIF-67-SO₄ crystals are composed of metal cobalt ions joined by imidazolate rings similar to Si and Al atoms coordinated by oxygens in zeolites. The key physicochemical properties such as high available surface area, porosity, surface charge, and unidirectional flow of electrons are particular parameters responsible for metronidazole adsorption by ZIF-67-SO₄. Developing hydrogen bonds between the nitrogen groups in MNZ and imidazolate rings and oxygen atoms, and also π -complexation between the cobalt ions and antibiotic rings are other mechanisms underlie the adsorption. In addition, the oxygen atom in the structure of MNZ is enough nucleophilic to bind with the metal species to form different coordination O–M configurations bonds.

Conclusion

The presence of antibiotics in the environment threatens human health and there is a substantial demand to control their discharges by promising treatment techniques such as adsorption. Metal–organic frameworks (MOFs) received tremendous interest in recent years due to their substantial structural properties. A unique member of MOFs namely ZIF-67-SO₄ employed as an adsorbent against the widely used antibiotic metronidazole (MNZ).

Kinetic model	parameter	value
	Concentration (mg/L)	25
Pseudo-first order		
$q_t = q_e(1 - e^{-k_1 t})$	q_e (mg/g)	25.36
	k_1 (min ⁻¹)	0.05
	R^2	0.97
	R^2_{Adj}	0.97
	RSS	9.95
	χ^2	1.99
Pseudo-second order		
$q_t = \frac{q_e^2 K_2 t}{1 + q_e K_2 t}$	q_e (mg/g)	33.38
	k_2 (g/mg min)	0.001
	R^2	0.98
	R^2_{Adj}	0.97
	RSS	8.25
	χ^2	1.65
Interparticle diffusion		
$q_t = k_3 \sqrt{t} + C$	k_3	3.24
	C	-0.06
	R^2	0.98
	R^2_{Adj}	0.98
	RSS	5.88
	χ^2	1.17

Table 7. The kinetic parameters for MNZ removal by ZIF-67-SO₄.

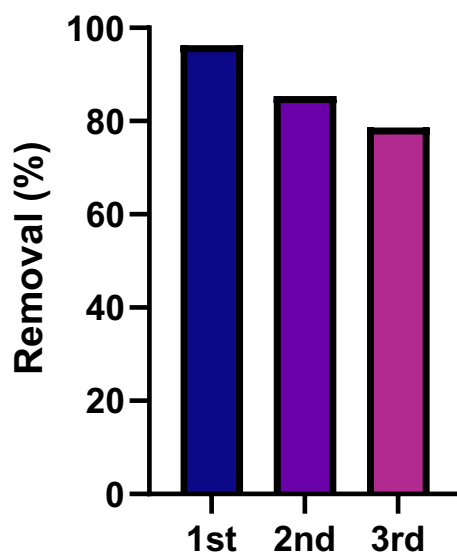


Figure 5. The reusability of ZIF-67-SO₄ for use-reuse system (ZIF-67-SO₄: 1g/L, pH=7, mixing time=60 min).

An in-depth study of the process accomplished by Box–Behnken design (BBD) to reveal the effects of significant variables and their interactions. A quadratic model was developed to predict and to optimize the process efficacy. The model predicted the highest MNZ removal of 97% occurs at pH=7, adsorbent dosage = 1 g/L, and mixing time = 60 min. MNZ removal was highest at near neutral pH and adsorbent mass was determined as the most influential variable in the process. Isotherm modeling indicated the MNZ adsorption followed the Langmuir isotherm with a $q_{max} = 63.03$ mg/g. ZIF-67-SO₄ also studied in three consecutive use-reuse systems with ~ 17.7% loss in adsorption efficiency.

Data availability

The datasets generated and analyzed during the current study were available from the corresponding author on reasonable request.

Received: 18 June 2023; Accepted: 30 August 2023

Published online: 05 September 2023

References

- Balouchi, H., Baziar, M., Dehghan, A., Alidadi, H. & Shams, M. Combination of electrocoagulation and MOF adsorption systems for EBT removal from water. *Int. J. Environ. Anal. Chem.* **102**, 1307–1317 (2022).
- Gurusamy, L., Anandan, S. & Wu, J. J. In *Metal-organic frameworks for chemical reactions* (eds Khan, A. et al.) 441–470 (Elsevier, 2021).
- Baziar, M. et al. Metal-organic and Zeolitic imidazole frameworks as cationic dye adsorbents: physicochemical optimizations by parametric modeling and kinetic studies. *J. Mol. Liq.* **332**, 115832. <https://doi.org/10.1016/j.molliq.2021.115832> (2021).
- Freund, R. et al. The current status of MOF and COF applications. *Angew. Chem. Int. Ed.* **60**, 23975–24001 (2021).
- Davoodi, M., Davar, F., Rezayat, M. R., Jafari, M. T. & Shalan, A. E. Cobalt metal-organic framework-based ZIF-67 for the trace determination of herbicide molinate by ion mobility spectrometry: Investigation of different morphologies. *RSC Adv.* **11**, 2643–2655 (2021).
- Duan, C., Yu, Y. & Hu, H. Recent progress on synthesis of ZIF-67-based materials and their application to heterogeneous catalysis. *Green Energy Environ.* **7**, 3–15. <https://doi.org/10.1016/j.gee.2020.12.023> (2022).
- Liu, N., Shang, S., Shi, D., Cheng, Q. & Pan, Z. Construction of hollow ZnO/Mn-ZIF-67 heterojunction photocatalysts: Enhanced photocatalytic performance and mechanistic insight. *New J. Chem.* **45**, 2285–2294 (2021).
- Shao, W. et al. Facile construction of a ZIF-67/AgCl/Ag heterojunction via chemical etching and surface ion exchange strategy for enhanced visible light driven photocatalysis. *RSC Adv.* **10**, 38174–38183 (2020).
- Afarinandeh, A. et al. Controlled removal of fluoride by ZIF-8, ZIF-67, and Ni-MOF of different morphologies. *Arab. J. Chem.* **16**, 104837. <https://doi.org/10.1016/j.arabjc.2023.104837> (2023).
- López-Cabrelles, J. et al. Solvent-free synthesis of ZIFs: A route toward the elusive Fe (II) analogue of ZIF-8. *J. Am. Chem. Soc.* **141**, 7173–7180 (2019).
- Phoon, B. L. et al. Conventional and emerging technologies for removal of antibiotics from wastewater. *J. Hazard. Mater.* **400**, 122961. <https://doi.org/10.1016/j.jhazmat.2020.122961> (2020).
- Alsubih, M. et al. Performance evaluation of constructed wetland for removal of pharmaceutical compounds from hospital wastewater: Seasonal perspective. *Arab. J. Chem.* **15**, 104344 (2022).
- Serwecińska, L. Antimicrobials and antibiotic-resistant bacteria: a risk to the environment and to public health. *Water* **12**, 3313 (2020).
- Yang, J., Wang, X., Zhu, M., Liu, H. & Ma, J. Investigation of PAA/PVDF–NZVI hybrids for metronidazole removal: Synthesis, characterization, and reactivity characteristics. *J. Hazard. Mater.* **264**, 269–277. <https://doi.org/10.1016/j.jhazmat.2013.11.037> (2014).
- Bonyadi, Z. et al. Biomass-derived porous aminated graphitic nanosheets for removal of the pharmaceutical metronidazole: Optimization of physicochemical features and exploration of process mechanisms. *Colloids Surf. A Physicochem. Eng. Asp.* **611**, 125791. <https://doi.org/10.1016/j.colsurfa.2020.125791> (2021).
- Esmaili, Z. et al. Biosorption of metronidazole using *Spirulina platensis* microalgae: Process modeling, kinetic, thermodynamic, and isotherm studies. *Appl. Water Sci.* **13**, 63. <https://doi.org/10.1007/s13201-023-01867-9> (2023).
- Awad, A. M. et al. Adsorption of organic pollutants by natural and modified clays: A comprehensive review. *Sep. Purif. Technol.* **228**, 115719 (2019).
- Baziar, M. et al. Metal-organic and Zeolitic imidazole frameworks as cationic dye adsorbents: Physicochemical optimizations by parametric modeling and kinetic studies. *J. Mol. Liq.* **332**, 115832 (2021).
- Kalhorizadeh, T. et al. Quick removal of metronidazole from aqueous solutions using metal-organic frameworks. *New J. Chem.* **46**, 9440–9450. <https://doi.org/10.1039/D1NJ06107K> (2022).
- Seo, P. W., Khan, N. A. & Jhung, S. H. Removal of nitroimidazole antibiotics from water by adsorption over metal-organic frameworks modified with urea or melamine. *Chem. Eng. J.* **315**, 92–100. <https://doi.org/10.1016/j.cej.2017.01.021> (2017).
- Alamgir, et al. Effective adsorption of metronidazole antibiotic from water with a stable Zr(IV)-MOFs: Insights from DFT, kinetics and thermodynamics studies. *J. Environ. Chem. Eng.* **8**, 103642. <https://doi.org/10.1016/j.jece.2019.103642> (2020).
- Haghighat, G. A., Gholikandi, G. B. & Mirabi, M. Removal of recalcitrant metronidazole from aqueous solution onto ZIF-8 & copper doped ZIF-8, process modelling and optimisation. *Int. J. Environ. Anal. Chem.* <https://doi.org/10.1080/03067319.2023.2185777> (2023).
- Guo, X., Xing, T., Lou, Y. & Chen, J. Controlling ZIF-67 crystals formation through various cobalt sources in aqueous solution. *J. Solid State Chem.* **235**, 107–112. <https://doi.org/10.1016/j.jssc.2015.12.021> (2016).
- Haghighat, G. A. et al. Aminated graphitic carbon derived from corn stover biomass as adsorbent against antibiotic tetracycline: Optimizing the physicochemical parameters. *J. Mol. Liq.* **313**, 113523. <https://doi.org/10.1016/j.molliq.2020.113523> (2020).
- Sparks, D. L. In *Environmental soil chemistry* 2nd edn (ed. Sparks, D. L.) 133–186 (Academic Press, 2003).
- Derakhshani, E., Naghizadeh, A. & Khodadadi, M. Application of different isotherm models for humic acid adsorption on to bentonite and montmorillonite nanoparticles. *Health Scope* **6** (2017).
- Ebelegi, A. N., Ayawei, N. & Wankasi, D. Interpretation of adsorption thermodynamics and kinetics. *Open J. Phys. Chem.* **10**, 166–182 (2020).
- Plazinski, W. & Rudzinski, W. Kinetics of adsorption at solid/solution interfaces controlled by intraparticle diffusion: a theoretical analysis. *J. Phys. Chem. C* **113**, 12495–12501 (2009).
- Mazloomi, S., Yousefi, M., Nourmoradi, H. & Shams, M. Evaluation of phosphate removal from aqueous solution using metal organic framework; isotherm, kinetic and thermodynamic study. *J. Environ. Health Sci. Eng.* **17**, 209–218 (2019).
- Zhang, S. et al. Zeolitic imidazole framework templated synthesis of nanoporous carbon as a novel fiber coating for solid-phase microextraction. *Analyst* **141**, 1127–1135. <https://doi.org/10.1039/C5AN02059J> (2016).
- Malepe, L., Ndinteh, T. D., Ndungu, P. & Mamo, M. A. A humidity-resistant and room temperature carbon soot@ZIF-67 composite sensor for acetone vapour detection. *Nanoscale Adv.* **5**, 1956–1969. <https://doi.org/10.1039/D3NA00050H> (2023).
- Dhaka, S. et al. Metal-organic frameworks (MOFs) for the removal of emerging contaminants from aquatic environments. *Coord. Chem. Rev.* **380**, 330–352. <https://doi.org/10.1016/j.ccr.2018.10.003> (2019).
- Zeng, Z.-W. et al. Comprehensive adsorption studies of doxycycline and ciprofloxacin antibiotics by biochars prepared at different temperatures. *Front. Chem.* **6**, 80 (2018).
- Alsaedi, M. K. et al. Antibiotic adsorption by metal-organic framework (UiO-66): A comprehensive kinetic, thermodynamic, and mechanistic study. *Antibiotics* **9**, 722 (2020).

35. Zong, Y. *et al.* Synthesis of porphyrin Zr-MOFs for the adsorption and photodegradation of antibiotics under visible light. *ACS Omega* **6**, 17228–17238 (2021).
36. Elkady, M., Diab, K. E. & Shokry, H. Trimethoprim antibiotic adsorption from aqueous solution onto eco-friendly zr-metal organic framework material. *Materials* **14**, 7545 (2021).
37. Aarab, N. *et al.* Experimental and DFT studies of the removal of pharmaceutical metronidazole from water using polypyrrole. *Int. J. Ind. Chem.* **10**, 269–279. <https://doi.org/10.1007/s40090-019-0190-7> (2019).
38. Onu, C. E. *et al.* Modeling, optimization, and adsorptive studies of bromocresol green dye removal using acid functionalized corn cob. *Clean. Chem. Eng.* **4**, 100067. <https://doi.org/10.1016/j.clce.2022.100067> (2022).
39. Dehghani, M. H., Afsari Sardari, S., Afsharnia, M., Qasemi, M. & Shams, M. Removal of toxic lead from aqueous solution using a low-cost adsorbent. *Sci. Rep.* **13**, 3278. <https://doi.org/10.1038/s41598-023-29674-x> (2023).
40. Sun, L., Chen, D., Wan, S. & Yu, Z. Adsorption studies of dimetridazole and metronidazole onto biochar derived from sugarcane bagasse: kinetic, equilibrium, and mechanisms. *J. Polym. Environ.* **26**, 765–777. <https://doi.org/10.1007/s10924-017-0986-5> (2018).
41. Nasseh, N., Barikbin, B., Taghavi, L. & Nasser, M. A. Adsorption of metronidazole antibiotic using a new magnetic nanocomposite from simulated wastewater (isotherm, kinetic and thermodynamic studies). *Compos. B Eng.* **159**, 146–156. <https://doi.org/10.1016/j.compositesb.2018.09.034> (2019).
42. Aslam, M. M. A. *et al.* In *Separation science and technology* Vol. 15 (ed. Ahuja, S.) 177–207 (Academic Press, 2022).
43. Wang, J. & Guo, X. Adsorption isotherm models: Classification, physical meaning, application and solving method. *Chemosphere* **258**, 127279 (2020).
44. Tzabar, N. & ter Brake, H. J. M. Adsorption isotherms and Sips models of nitrogen, methane, ethane, and propane on commercial activated carbons and polyvinylidene chloride. *Adsorption* **22**, 901–914. <https://doi.org/10.1007/s10450-016-9794-9> (2016).
45. Oni, B. A., Sanni, S. E., Agu, K. C. & Tomomewo, O. S. Green synthesis of Ag nanoparticles from *Argemone mexicana* L. leaf extract coated with MOF-5 for the removal of metronidazole antibiotics from aqueous solution. *J. Environ. Manag.* **342**, 118161. <https://doi.org/10.1016/j.jenvman.2023.118161> (2023).
46. Parashar, D., Harafan, A., Achari, G. & Kumar, M. Ciprofloxacin and metronidazole adsorption on chitosan-modified graphene oxide as single-compound and binary mixtures: Kinetics, isotherm, and sorption mechanism. *J. Hazard. Toxic Radioact. Waste* **27**, 04022042 (2023).
47. Krstić, V. In *Handbook of nanomaterials for wastewater treatment* (eds Bhanvase, B. *et al.*) 417–481 (Elsevier, 2021).
48. Girish, C. & Murty, V. R. Mass transfer studies on adsorption of phenol from wastewater using *Lantana camara*, forest waste. *Int. J. Chem. Eng.* **2016** (2016).

Acknowledgements

A special thanks to the Ilam University of Medical Sciences, Ilam, Iran for its financial support under the Grant # 994017/111.

Author contributions

S.M.: Conceptualization, Methodology, Investigation, Formal analysis, Writing—original draft. A.A., F.G., G.A.H., G.B.G., H.N., M.F., B.N.L.: Investigation, Methodology, Writing—review & editing. A.A.M.: Methodology, Writing—review & editing, Supervision.

Competing interests

The authors declare no competing interests.

Additional information

Supplementary Information The online version contains supplementary material available at <https://doi.org/10.1038/s41598-023-41724-y>.

Correspondence and requests for materials should be addressed to A.A.M. or M.F.

Reprints and permissions information is available at www.nature.com/reprints.

Publisher's note Springer Nature remains neutral with regard to jurisdictional claims in published maps and institutional affiliations.



Open Access This article is licensed under a Creative Commons Attribution 4.0 International License, which permits use, sharing, adaptation, distribution and reproduction in any medium or format, as long as you give appropriate credit to the original author(s) and the source, provide a link to the Creative Commons licence, and indicate if changes were made. The images or other third party material in this article are included in the article's Creative Commons licence, unless indicated otherwise in a credit line to the material. If material is not included in the article's Creative Commons licence and your intended use is not permitted by statutory regulation or exceeds the permitted use, you will need to obtain permission directly from the copyright holder. To view a copy of this licence, visit <http://creativecommons.org/licenses/by/4.0/>.

© The Author(s) 2023